Conference of the Japan Society of Microgravity Application

PS15

液柱内温度差マランゴニ対流における電場印加が帯電粒子挙動に与える影響

Effect of Applied Electric Field on the Behavior of Charged Particles in Thermocapillary Convection of a Liquid Bridge

吉田優人 [1], 石村美紗 [2], 西野耕一 [2],
Yuto YOSHIDA[1], Misa ISHIMURA[1] and Koichi NISHINO[2]
[1] 横浜国立大学大学院，Graduate School, Yokohama National University
[2] 横浜国立大学，Yokohama National University

1. Introduction

A floating zone (FZ) method[1)] is used for generating high-purity single crystals of silicon. In the molten section, natural convection has an adverse effect on crystal growth. To suppress this effect, experiments of the FZ method were conducted under microgravity. However, Marangoni convection, driven by surface tension differences, became dominant. This convection is known to adversely affect crystal growth. Therefore, it is important to better understand Marangoni convection and thereby manipulate it. So far, experiments have been conducted using a liquid bridge, where a liquid is suspended between two cylindrical disks. In previous studies, Marangoni convection due to temperature difference in the liquid bridge was controlled by heating or applying a magnetic field[2,3)]. Although convection control by electric field is expected in industrial applications due to its controllability and non-contact application, there are yet few studies[4)] on the effect of electric field on Marangoni convection in a liquid bridge. Furthermore, it is known that the application of an electric field changes the surface tension and causes the EHD effect, but the principle of EHD generation in a liquid bridge and the dependence of the surface tension on the electric field have not yet been clarified.

In experiments on Marangoni convection, particle image velocimetry (PIV) is a powerful tool for visualizing flow field, where we can analyze the flow field by capturing images of tracer particles injected into the fluid. It has been demonstrated[5)] that the particle motion accurately represents the fluid motion in the case where a small temperature difference is applied to the liquid bridge. On the other hand, when an electric field is applied to the liquid bridge, the particles are observed to be driven by the electric field, suggesting that the particles are electrically charged[6-9)]. This effect must be clarified in order to determine whether the application of an electric field contributes to the convection control or simply affects the particle motion (or results in both). Therefore, understanding the effect of charged particles is essential for evaluating convection control by an electric field. The present study aims at conducting numerical analyses with a view to understanding how and to what extent charged particles affect the flow field and flow visualization.

2. Numerical analysis

Numerical simulations were performed using the commercial CFD solver STAR-CCM+. The computational domain consists only of a liquid bridge suspended between the two concentric disks as shown in **Figure 1**, where electrically charged particles exists in the fluid. A two-dimensional unsteady analysis is performed assuming axisymmetric flow and no deformation of the liquid bridge. Flow conditions and physical properties of the fluid are the same as those of ground experiments conducted by Yamazaki[7)]. He carried out a series of PIV analysis of the motion of nylon 12 particles in 5 cSt silicone oil where temperature and potential differences were applied between two disks. The physical properties assumed in the present numerical simulation are summarized in **Table 1**, where the one-way coupling between particles and fluid is assumed and only charged particles are affected by the applied electric field. By performing the analysis based on this assumption, the effect of applied electric field on the behavior of charged particles is clarified.

The governing equations for fluids are obtained from the conservation of mass, momentum and energy:

$$\nabla \cdot \boldsymbol{u} = 0, \tag{1}$$

$$\frac{\partial \boldsymbol{u}}{\partial t} + (\boldsymbol{u} \cdot \nabla)\boldsymbol{u} = -\frac{1}{\rho}\nabla p + \nu \nabla^2 \boldsymbol{u} + \boldsymbol{f_b}, \tag{2}$$

$$\frac{\partial T}{\partial t} + (\boldsymbol{u} \cdot \nabla)T = \alpha \nabla^2 T, \tag{3}$$

where $\boldsymbol{u}$ is the fluid velocity, t is the time, ρ is the density, p is the pressure, ν is the kinematic viscosity, $\boldsymbol{f_b}$ is the body force such as buoyancy and Marangoni force, T is the temperature, and α is the thermal diffusivity.

Marangoni force is considered using Tiwari & Nishino's method[10)], which mimics a surface force as a body force acting on a thin surface cell:

$$F_m = \sigma_T \frac{\partial T}{\partial z}\frac{1}{\delta r}, \tag{4}$$

where σ_T is the temperature coefficient of surface tension , and δr is the surface cell thickness.

The Lagrangian method is used for the calculation of particle motion. Different from the Eulerian fluid calculations solved by the finite volume method, the governing equations are defined for each individual particle. The governing equation for particles is obtained from the conservation of momentum and these are the forces acting on the particles:

$$m_p \frac{d\boldsymbol{u_p}}{dt} = \boldsymbol{F_s} + \boldsymbol{F_b}, \tag{5}$$

$$\boldsymbol{F_s} = \boldsymbol{F_d} + \boldsymbol{F_p} + \boldsymbol{F_{LS}}, \tag{6}$$

$$\boldsymbol{F_b} = \boldsymbol{F_g} + \boldsymbol{F_{Co}}, \tag{7}$$

where m_p is the particle mass, $\boldsymbol{v_p}$ is the particle velocity, $\boldsymbol{F_s}$ is the surface force, $\boldsymbol{F_b}$ is the body force, $\boldsymbol{F_d}$ is the drag force, $\boldsymbol{F_p}$ is the pressure gradient force, $\boldsymbol{F_{LS}}$ is the shear lift force, $\boldsymbol{F_g}$ is the gravitational force, and $\boldsymbol{F_{Co}}$ is the coulomb force.

These are the boundary conditions at the free surface, top disk, and bottom disk:

$$u_r = 0, \frac{\partial T}{\partial r} = 0, \frac{\partial \phi}{\partial r} = 0 \ (r = R), \tag{8)\sim(10}$$

$$u_r = 0, u_z = 0, \mathrm{T} = T_h, \phi = \Delta E \ (\mathrm{z} = H), \tag{11)~(14}$$

$$u_r = 0, u_z = 0, \mathrm{T} = T_c, \phi = 0 \ (\mathrm{z} = 0), \tag{15)~(18}$$

where u_r is the radial velocity, R is the radius of the liquid bridge, u_z is the axial velocity, H is the height of the liquid bridge, and ϕ is the electric potential.

In this study, the analysis is performed for 5 different particle charges of $q_p = 0, 1, 4.42, 10, 24.8 \times 10^{-17}$ C. The Pauthenier equation for the saturation charge due to the electric field charge is calculated as

$$q_\infty = 12\pi\varepsilon_p {R_p}^2 |\boldsymbol{E}| / \left(\frac{\varepsilon_p}{\varepsilon_0} + 2\right), \tag{19}$$

where ε_p is the particle permittivity, R_p is the particle radius, $\boldsymbol{E}$ is the electric field intensity, and ε_0 is the vacuum permittivity. This gives $q_\infty = 24.8 \times 10^{-17}$ C. In addition, unpublished internal data from our laboratory[11)] shows $q_{exp} = 4.42 \times 10^{-17}$ C, obtained from an experiment in which an electric field was applied to a liquid bridge without a free surface and the amount of charge was estimated from particle movement. However, this value contains errors and should be treated with caution. Since it is not currently possible to accurately measure the particle charge, $q_\infty = 0, 1, 10 \times 10^{-17}$ C are added, and 5 different charge values are used to evaluate the particles under a wide range of charging conditions.

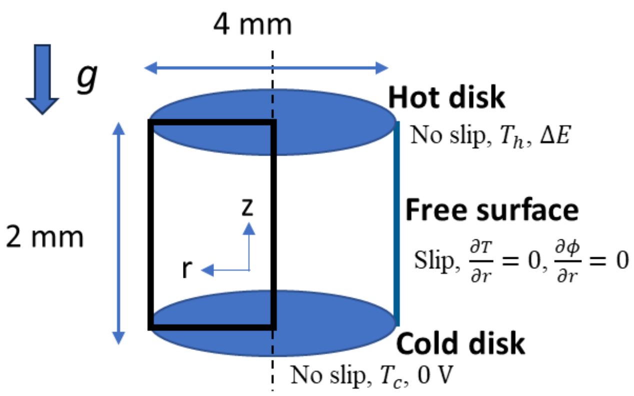

Figure 1. Geometry of the analytical liquid bridge.

Table 1. Physical properties of silicone oil and nylon 12 particles.

Silicone oil [a]		Nylon 12 particles [b]	
Kinematic viscosity [cSt]	5	**Average particle size [μm]**	5.0
Density [kg/m³]	915	**Feature**	Spherical
Specific heat [J/(kg*K)]	1.8×10^3	**Density [kg/m³]**	1016.94
Permittivity [F/m]	2.6×10^{-11}	**Permittivity [F/m]**	3.72×10^{-11}
Temperature coefficient of surface tension [N/(m*K)]	-6.58×10^{-5}	**Particle charge [C]**	$0, 1, 4.42, 10, 24.8 \times 10^{-17}$

3. Results and discussion

Figure 2 shows the velocity vectors of the fluids and charged particles ($q_p = 4.42 \times 10^{-17}$ C) in the electric field. Twenty thousand particles were initially introduced at equal intervals, and the velocity vectors of fluid and particles at 3 [s] after the application of the electric field are indicated. The conditions are as follows: temperature difference (ΔT) of 10 [°C] and the potential difference (ΔE) of 400 [V] between the top and bottom of the liquid bridge. The temperature and electric potential distributions of the fluid are shown in **Figure 3**. These results are the left half of the cross section of the liquid bridge. From **Figure 2**, it is recognized that both fluid and particles show similar velocity vectors in that they flow downward near the free surface and flow upward near the axis but that their quantitative distributions are appreciable different as discussed in detail below.

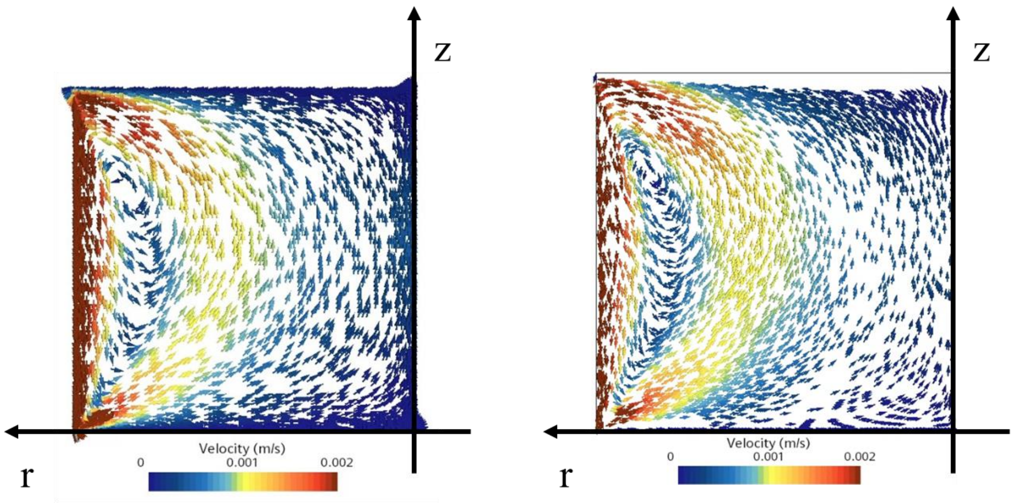

[a] Fluid [b] Charged particles

Figure 2. Velocity vectors of fluid and charged particles, where the left and right boundaries of each figure are the free surface and the axis of the liquid bridge, respectively.

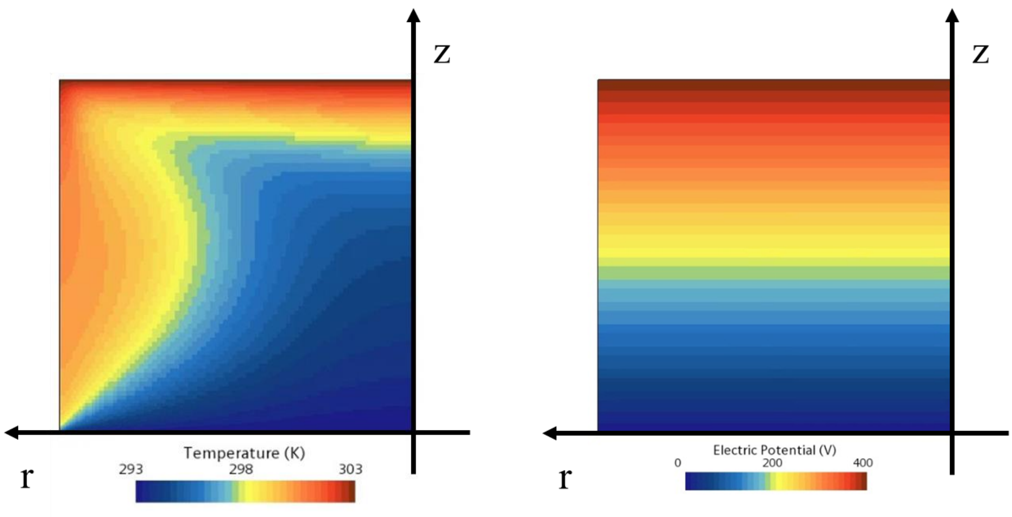

[a] Temperature [b] Electric potential

Figure 3. Temperature and electric potential distributions.

Figure 4 shows the histograms of the particle slip velocity, $\boldsymbol{u}_{\mathbf{slip}} = \boldsymbol{u} - \boldsymbol{u}_{\mathbf{p}}$, where **Figure 4-1** gives those for no-charged particles while **Figure 4-2** gives those of charged particles ($q_p = 4.42 \times 10^{-17}$ C). Each figure shows the particle slip velocities in axial and radial directions. In the absence of charge, the slip velocity is distributed around 0 mm/s for both axial and radial directions. Although not shown here, the slip velocity between fluid and ideal particles (i.e., sufficiently small particles having fluid density) is found to be quite similar to that shown in **Figure 4-1**, therefore indicating that the slip velocity distribution seen here is caused by the Lagrangian method used in the present numerical analysis. This must be considered in the interpretation of the slip velocity between charged particles and fluid. Under the charged condition, the axial slip velocity is distributed around 0.04 mm/s. This is because the charged particles are attracted in the direction of the cathode by the applied electric field. When comparing the kurtosis k of the $u_{\mathrm{slip}(z)}$, $k = 126$ for $q_p = 0$ C and $k = 46$ for $q_p = 4.42 \times 10^{-17}$ C, indicating that the distribution for the charged particles has lower peak value. In the previous study by Kimura and Kamii[12)], the ratio between the moving body's relative velocity under oscillatory flow and the terminal velocity in a stationary fluid, $\frac{\boldsymbol{u}_{\mathbf{slip}}}{\boldsymbol{u}_{\mathbf{ter}}}$, is greater than 0.99 under the conditions of the density ratio of 1.5 and the particle diameter of 2 mm. Their study suggests that for particles of small diameter and near-fluid density, the oscillatory flow has no effect on the terminal velocity of the particles. Furthermore, they showed that the particle velocity is represented by the superposition of the velocity of the oscillatory flow and the terminal velocity estimated for the stationary fluid. If this superposition is applicable to the present study, the slip velocity should be calculated using Stokes' law:

$$\boldsymbol{u}_{ter} = \frac{\boldsymbol{F}_q}{6\pi\mu R_p} = \frac{q_p\boldsymbol{E}}{6\pi\mu R_p} = 0.041\ mm/s, \tag{20}$$

where μ is the fluid viscosity. This terminal velocity can explain the peak velocity of $u_{\mathrm{slip}(z)}$ seen in **Figure 4-2**. However, it also shows that it is widely distributed around the terminal velocity. This is because the drag force on the particles changes as the fluid velocity differs from place to place in the liquid bridge, resulting in a wide range of slip velocity. Therefore, the superposition of thermocapillary convection and particle terminal velocity cannot represent particle behavior.

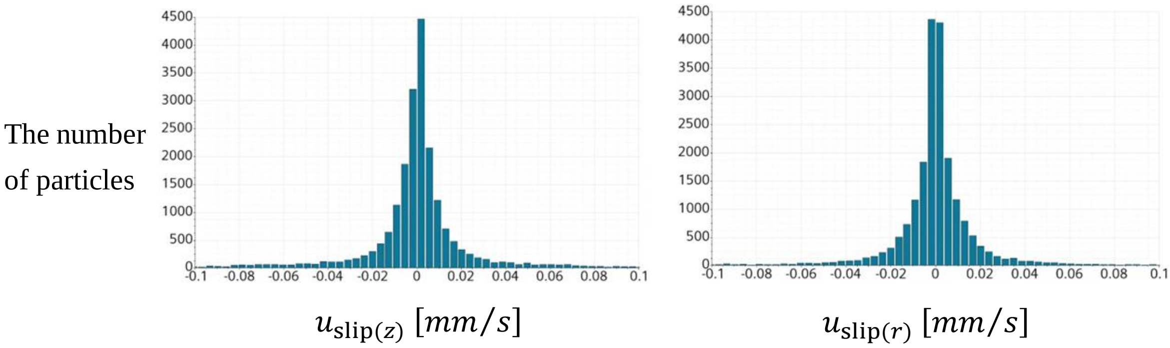

Figure 4-1. Histogram of particle slip velocity without charge.

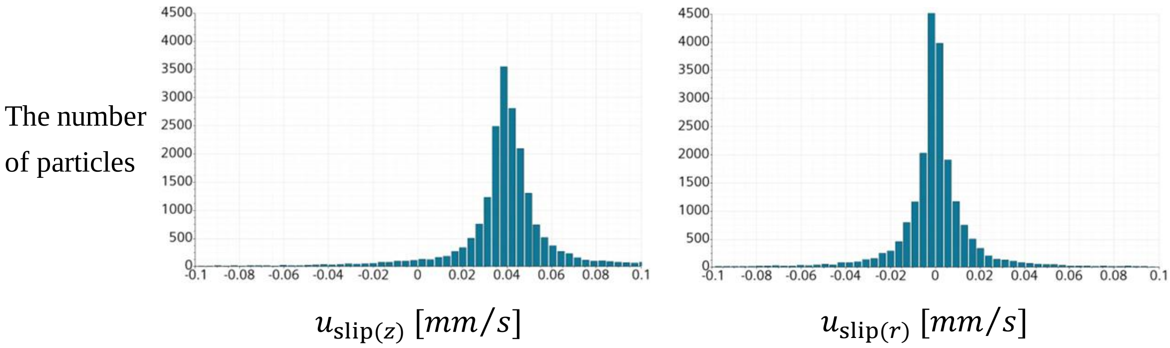

Figure 4-2. Histogram of particle slip velocity for $q_p = 4.42 \times 10^{-17}$ C.

To evaluate particle traceability, the ratio of particle velocity to flow velocity, $\frac{u_{p(z)}}{u_{(z)}}$, has been defined here. **Figure 5** shows histograms of $\frac{u_{p(z)}}{u_{(z)}}$ at particle charges $q_p = 0, 1, 4.42, 10, 24.8 \times 10^{-17}$ C. When $q_p = 0$ C, there are many particles with $\frac{u_{p(z)}}{u_{(z)}}$ close to 1, indicating good fidelity as fluid tracers. This indicates that the particles follow the flow well under conditions where there is no electrical influence on the particles, such as when the particles are not charged or when only a temperature difference is applied without applying an electric field, due to their small particle size and the slight difference in density between particles and fluids. On the other hand, as the charge increases, the number of particles with $\frac{u_{p(z)}}{u_{(z)}}$ values away from 1 increases and their distribution becomes wider. Additionally, for $q_p = 4.42 \times 10^{-17}$ C or higher, there are many particles with poor fidelity. Therefore, when selecting particles as tracer particles for PIV, it is necessary to consider their charging characteristics. The degree of goodness as fluid tracers can be evaluated as how many particles out of all particles injected into the computational domain have a $\frac{u_{p(z)}}{u_{(z)}}$ value that can be considered indicative of good fidelity. The ranges for good fidelity are examined as 0.9~1.1, 0.95~1.05, and 0.99~1.01, respectively, but 0.95~1.05, which is widely used as the standard, is used in this study. **Figure 6** shows the particle distribution of $\frac{u_{p(z)}}{u_{(z)}}$ for each charge amount. From left to right, particles satisfying $0.95 < \frac{u_{p(z)}}{u_{(z)}} < 1.05$ (good fidelity) and $\frac{u_{p(z)}}{u_{(z)}} < 0.95$ or $1.05 < \frac{u_{p(z)}}{u_{(z)}}$ (poor fidelity) are displayed. In the case of no charge, most of the flow field is occupied by particles with good fidelity, whereas, at $q_p = 4.42 \times 10^{-17}$ C, particles with poor fidelity are more widely distributed. This indicates that the applied electric field deteriorates particle fidelity. **Figure 7** shows the ratio of particles with good tracking performance on the vertical axis and the amount of charge on the horizontal axis, and also shows a least-squares fitting curve. From this curve, it can be seen that in order for more than 70% of the particles to satisfy $0.95 < \frac{u_{p(z)}}{u_{(z)}} < 1.05$, the amount of charge must be kept below $q_p = 2.03 \times 10^{-17}$ C, and for more than 80% of the particles to satisfy it, the amount of charge must be kept below $q_p = 0.95 \times 10^{-17}$ C. Therefore, when using PIV particles in liquid bridge experiments involving the application of an electric field, the particles should be used within a good tracking range considering their charging characteristics.

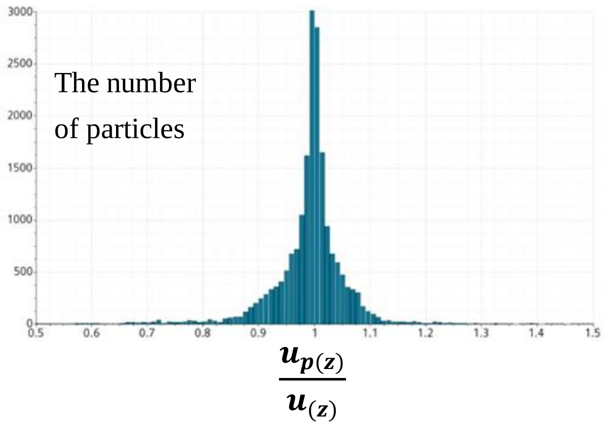

$q_p = 0$ C

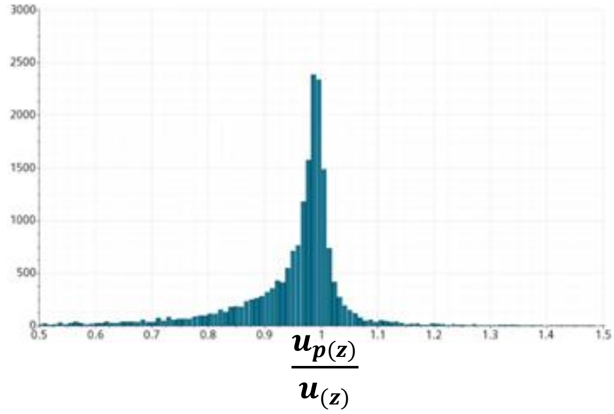

$q_p = 1 \times 10^{-17}$ C

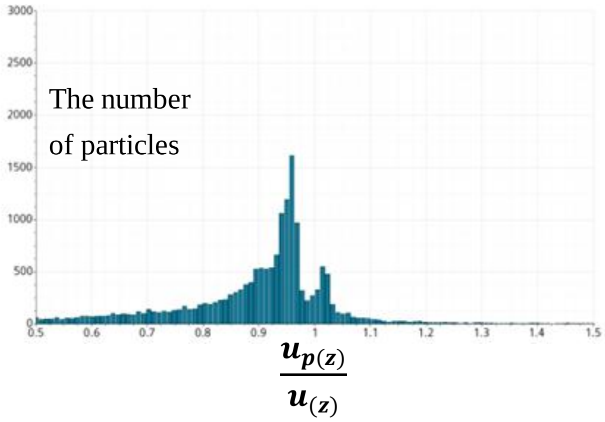

$q_p = 4.42 \times 10^{-17}$ C

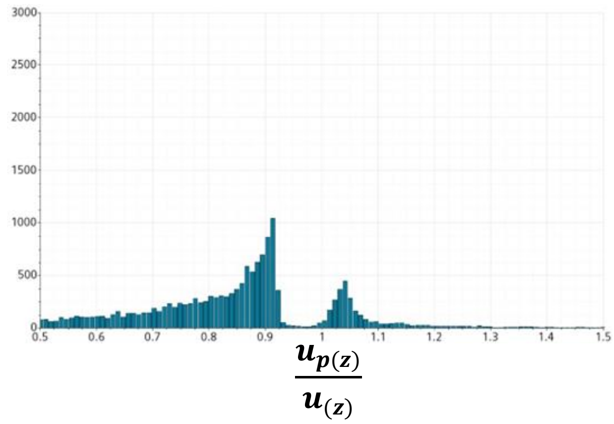

$q_p = 10 \times 10^{-17}$ C

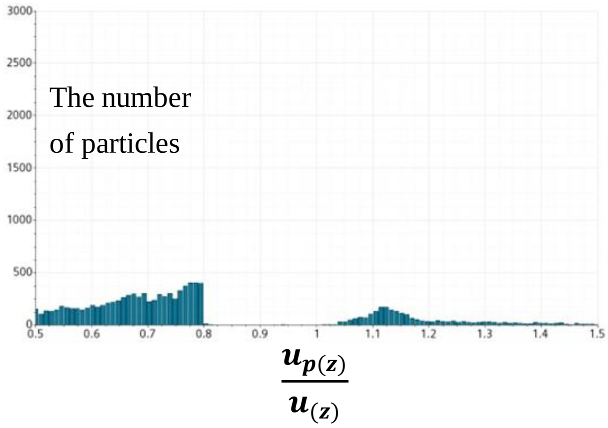

$q_p = 24.8 \times 10^{-17}$ C

Figure 5. Histograms of $\frac{u_{p(z)}}{u_{(z)}}$ at $q_p = 0, 1, 4.42, 10, 24.8 \times 10^{-17}$ C.

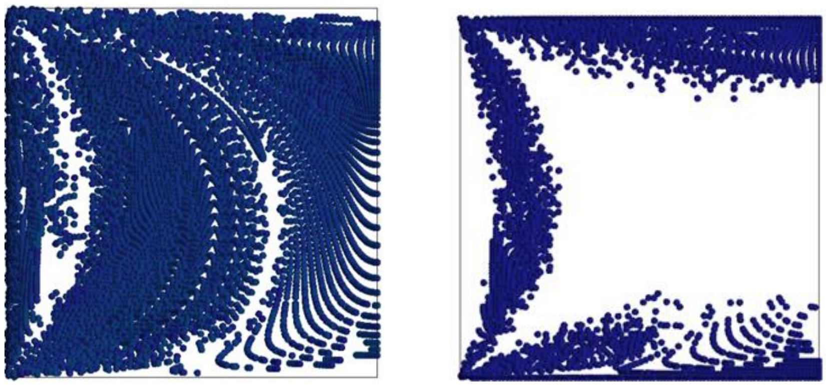

[a] Good fidelity [b] Poor fidelity

Figure 6-1. The distribution of $\frac{u_{p(z)}}{u_{(z)}}$ for $q_p = 0\ \mathrm{C}$ (good and poor fidelity).

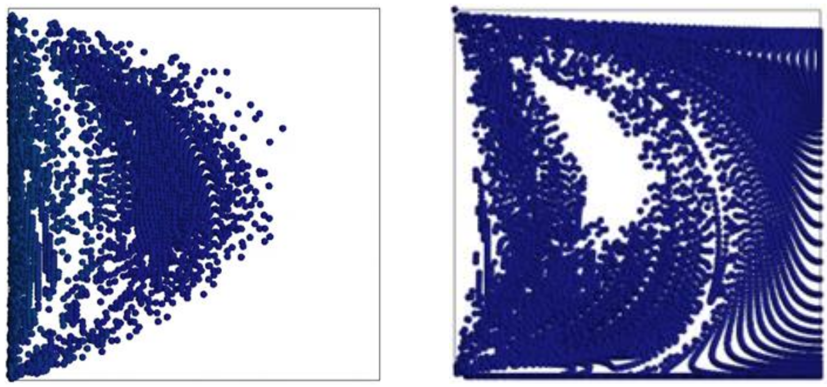

[a] Good fidelity [b] Poor fidelity

Figure 6-2. The distribution of $\frac{u_{p(z)}}{u_{(z)}}$ for $q_p = 4.42\ \times 10^{-17}\ \mathrm{C}$ (good and poor fidelity).

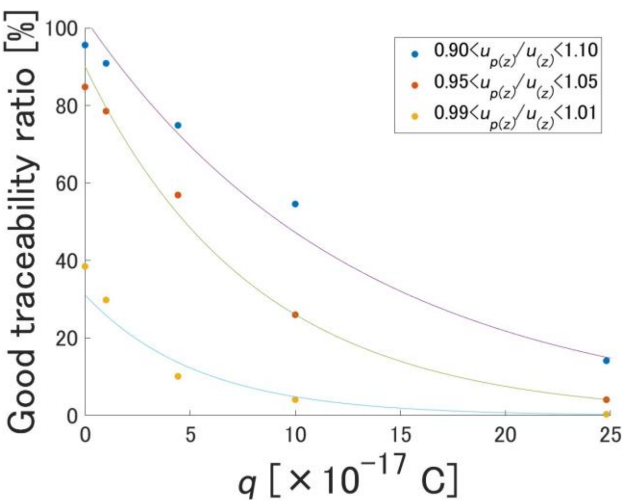

Figure 7. The ratio of the good tracer particle

4. Conclusions

The effect of applied electric field on the charged particles in thermocapillary convection in a liquid bridge has been investigated by numerical analysis based on the Lagrangian method for particle behavior. By changing the charge quantity and by examining the velocity and the number of particles, the following findings were obtained.

1) Slip velocities are not constant but distributed around the terminal velocity due to the electrical force. This suggests that the particle behaviors cannot simply be represented by the superposition of fluid flow and terminal velocity evaluated for stationary fluid.

2) Increasing particle charge shifts $\frac{u_{p(z)}}{u_{(z)}}$ value away from 1 and broadens the distribution.

3) The choice of tracer particles considering their charging characteristics is important for the experiment of thermocapillary convection in a liquid bridge exposed to an electric field.

References

1) P.H. Keck and M. J. E. Golay: Crystallization of silicon from a floating liquid zone. Phys. Rev, **89** (1953) 1297, DOI: https://doi.org/10.1103/PhysRev.89.1297.
2) M. Kudo and H. Kawamura: Control of Oscillatory Thermocapillary Convection in a Half-Zone Liquid Bridge by Circumferential Round Heating. Thermal Science & Engineering, **14** (2006) 19, DOI: https://doi.org/10.11368/tse.14.19.
3) Y. Tsutsumida, H. Minakuchi, Y. Takagi, Y. Okano and S. Gima: Effects of magnetic fields on Marangoni convection in a floating half-zone. The Japan Society of Mechanical Engineers, **25** (2012) 118, DOI: https://doi.org/10.1299/jsmecmd.2012.25.118.
4) M. Haga, T. Maekawa, K. Kuwahara, A. Ohara, K. Kawasaki, T. Harada, S. Yoda and T. Nakamura: Effect of Electric Field on Marangoni Convection under Microgravity. J. Jpn. Soc. Microgravity Appl., **12** (1995) 19, DOI: https://doi.org/10.15011/jasma.12.1.19
5) T. Yano, K. Nishino, H. Kawamura, I Ueno, S. Matsumoto, M. Ohnishi, M. Sakurai: 3-D PTV measurement of Marangoni convection in liquid bridge in space experiment. Experiments in fluids, **53** (2012) 9, DOI: https://doi.org/10.1007/s00348-011-1136-9.
6) K. Yamazaki: The study of the effect of an electric field on thermocapillary flow in a hanging droplet. Master's thesis, Yokohama National University (2019).
7) K. Yamazaki: Behavior of liquid bridge Marangoni convection under temperature field and electric field. Graduation thesis, Yokohama National University (2021).
8) C. Matsuno: Electrocapillary convection in the liquid film by electric dependence of surface tension. Master's thesis, Yokohama National University (2022).
9) K. Yamazaki: Electric field dependence of surface tension in dielectric fluids and Marangoni convection in thin liquid film due to external electric field. Master's thesis, Yokohama National University (2023).
10) S. Tiwari and K. Nishino: Numerical study to investigate the effect of partition block and ambient air temperature on interfacial heat transfer in liquid bridges of high Prandtl number fluid. J. Cryst. Growth, **300** (2007) 486, DOI: https://doi.org/10.1016/j.jcrysgro.2006.12.049.
11) K. Yamazaki, a private letter.
12) H. Kimura and Y. Kamii: Dynamic Forces of Fluid Acting on a Moving Body in Unsteady Flow Field and Motion of Sinking Matter. Fisheries Engineering, **50** (2013) 1, DOI: https://doi.org/10.18903/fisheng.50.1_1.

© 2024 by the authors. Submitted for possible open access publication under the terms and conditions of the Creative Commons Attribution (CC BY) license (http://creativecommons.org/li censes/by/4.0/).